Photoelectron spectroscopy studies of growth, alloying, and segregation for transition-metal films on tungsten (211)

J. J. Kolodziej* and T. E. Madey†

The Department of Physics and Astronomy and Laboratory for Surface Modification, Rutgers, The State University of New Jersey, Piscataway, New Jersey 08854-8019

J. W. Keister and J. E Rowe

Physics Department, North Carolina State University, Raleigh, North Carolina 27695

High resolution soft x-ray photoelectron spectroscopy using synchrotron radiation and Auger-electron spectroscopy are used to study late-transition-metal films (Pt, Pd, Ir, Rh, Au,) on W(211). It is found that the films grow in a layer mode at 300 K. As a function of the film thickness, different $4f_{7/2}$ photoemission peaks are observed, corresponding to a single monolayer, to an interface layer, to bulk atoms and to surface atoms. Single physical monolayers of these late-transition metals on tungsten are stable against thermal rearrangement. In contrast, when multilayer films of Pd, Pt, Ir, Rh are annealed above 700–1000 K, tungsten atoms diffuse into the overlayer to form an alloy film. Gold constitutes a different case; upon annealing it does not alloy with tungsten but the metal in excess of one monolayer forms clusters. The evolution of the bimetallic systems as a function of coverage and annealing temperature is interpreted by analysis of intensities and shapes of the $4f_{7/2}$ features. Born-Haber cycles and the equivalent core approximation are used to extract thermochemical data concerning energetics of adhesion, segregation, and alloying in these early-late transition-metal systems.

I. INTRODUCTION

It has been shown recently that the atomically rough tungsten (111) surface undergoes morphological changes upon adsorbing monolayer films of certain metals (Pt, Pd, Ir, Rh, Au), followed by annealing to $T>750$ K.[1,2] Under these conditions, the metal film-coated W(111) becomes covered with three-sided pyramids of nanometer scale dimensions, having {211} planes as facet sides. Because of the special role of W{211} planes in the faceting process, the goal of the present paper is to provide detailed information on growth, segregation, and alloying processes occurring on W(211)-based bimetallic systems involving late transition metals, as well as on the electronic properties of these systems. A preliminary study of metals on W(211) has appeared recently,[3] and a comparative study for metal films on a W(111) substrate is currently in preparation.[4]

Bimetallic systems have attracted much attention recently, both because they have interesting physical properties,[5] and because of the variety of their technological applications as catalysts, shape memory alloys, and new magnetic materials. Transition-metal films and alloys have a complex valence-band structure arising from hybridized s, p, and d bands. High densities of electronic states, both below and above the Fermi level, are available for bonding, making them ideal candidates for model catalysts and for adsorption studies. The analysis of bimetallic system properties is, however, not an easy task for the experimentalist; when one metal is deposited on another, many different phenomena are possible. The deposited metal atoms may stick where they hit, or may diffuse to form two- or three-dimensional islands on the surface. They may also dissolve into the substrate to form a surface or bulk alloy, or the substrate atoms may diffuse into

the deposited film. The wealth of possible phenomena makes the interpretation of experimental data rather difficult and the experimental techniques employed must distinguish between atoms in different configurations (i.e., atom on surface, impurity atom, alloy, etc.) Despite many challenges with data interpretation, high resolution soft x-ray photoelectron spectroscopy (SXPS) using synchrotron radiation is an extremely useful technique for studies of bimetallic interfaces; SXPS often provides identification of the surroundings of various atoms via measurements of core-level shifts, even if it is not possible to fully understand the physical origin of the peak shift. In the present work the SXPS technique is used to study processes which take place during growth and annealing of late transition-metal films (Pt, Pd, Ir, Rh, Au) on the tungsten (211) surface. Film growth processes and the formation of ordered surface structures are determined using Auger electron spectroscopy and low-energy electron diffraction (LEED), respectively.

The aspect of SXPS most relevant to the present work is the fact that core-level electron binding energies in an atom reflect the chemical environment of the atom.[6] If the atom is embedded in a solid, these energies are a function of the valence electronic structure of the solid. For many ionic and covalent compounds where interatomic charge transfer is substantial, the initial-state core-level shifts are accompanied by parallel shifts in positions of x-ray photoelectron spectroscopy peaks. However, for bimetallic systems, such as monolayer films or alloys where interatomic charge transfer is often not significant, the photoelectron peak shifts are influenced by several additional effects. These effects include final-state screening changes, intra-atomic charge transfer and reference level changes.[7] Understanding the physical origins of the shifts requires referring them to the absolute en-

ergy level, and the separation of initial and final-state effects. This is a very complex task and often it is not possible to carry it out other than by detailed electronic structure calculations.

An alternative approach to understanding core-level shifts on metals which circumvents these difficulties was proposed by Johannssen and Martensson[8] and by Steiner and Hufner,[9] and is based on Born-Haber cycles and the equivalent core approximation (ECA). It was shown that core-level shifts could be related to thermochemical properties of metals and alloys such as segregation, adhesion, and solution energies. This approach is used in the present work to extract thermochemical data for studied systems.

This paper is organized as follows. After the description of experimental procedures we present results and data analysis for five different metallic overlayers (Pt, Pd, Ir, Rh, Au) on W(211); as indicated above, all of these metals are known to induce faceting of W(111) to {211}. The Pt/W(211) data are described in greatest detail to illustrate the analysis and curve-fitting procedures. The essential features of the remaining four overlayers are presented more briefly. Finally, all of the data are discussed in terms of film growth, thermal stability, and alloy formation. A particularly interesting conclusion is that single monolayers of deposited metal on W(211) are thermally stable upon annealing, whereas ultrathin film alloys can form for overlayer deposits of Pt, Pd, Ir, Rh in excess of one monolayer.

II. EXPERIMENTAL METHODS

The experiments have been performed in stainless steel ultrahigh vacuum experimental systems at the National Synchrotron Light Source (NSLS) of Brookhaven National Laboratory, on beamline U4A, and at the Laboratory for Surface Modification at Rutgers University. The experimental chambers have base pressures of less than 1×10^{-10} Torr.

The NSLS setup is connected to the storage ring via a six-meter toroidal grating monochromator providing synchrotron radiation in the range 10–200 eV. Photoelectron spectra have been measured with a 100-mm VSW hemispherical analyzer. The total spectral resolution is better than 0.2 eV at 150 eV and below 0.1 eV at 80 eV photon energy. The x-ray beam and the energy spectrometer axis form an angle of 45° and the x-ray beam is in most cases incident at 45° onto the sample. The photon flux is monitored and the measured spectra are normalized to account for slowly changing photon flux.

The Rutgers system contains instrumentation for Auger electron spectroscopy (AES), low-energy electron diffraction (LEED), and a quartz crystal microbalance (QCM). Both systems also contain several metal dosers used for deposition of platinum, palladium, rhodium, iridium, and gold. The tungsten (211) substrate is prepared by heating in oxygen (1×10^{-7} Torr) at 1300 K, followed by an abrupt increase of substrate temperature to 2300 K for a few seconds. The cycle is repeated until no traces of carbon can be found in AES spectra. Following this treatment the tungsten sample rarely needs oxygen treatment, and it can be cleaned by high-temperature flashes only. Metal dosers are constructed by wrapping thin metal wires (0.1–0.25 mm for Au, Rh, and Pd) around a resistively heated tungsten filament or by spot-
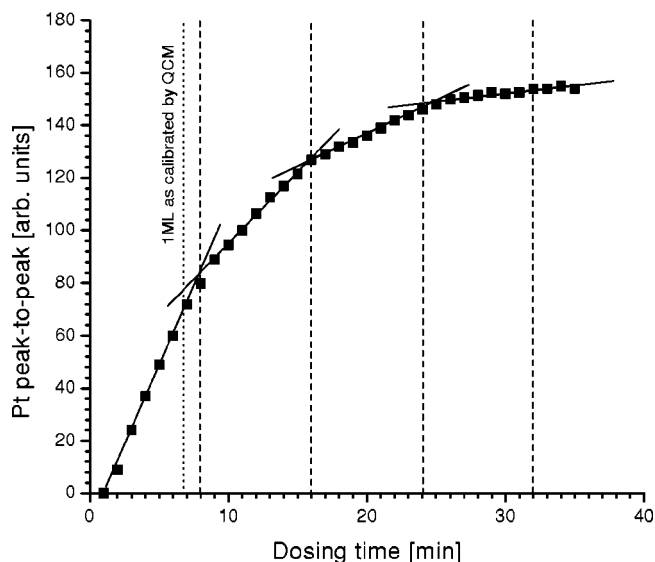
FIG. 1. Pt Auger signal intensity (at 64 eV, peak to peak) as a function of dosing time for Pt growth on W(211) at 300 K.

welding a piece of foil (Pt) to a tungsten wire. The Ir source is a resistively heated Ir filament. Special care is taken to outgas the dosers before their use. Dosers are shielded during operation by cooled surfaces and the background pressure during dosing does not exceed 2×10^{-10} Torr.

Although admetal photoelectron peak shapes provide an accurate way to calibrate the dosing rate, a variety of different techniques is used throughout the related experiments in order to cross check surface coverages. Complementary methods for surface coverage calibration include the QCM, Auger uptake curves, change in work function, and temperature programmed desorption. The details of the coverage calibration are discussed elsewhere.[3]

In order to investigate thermally activated processes occuring on overlayer films and at the interface, stepwise annealing to increasingly higher temperatures is used: after metal deposition, the sample is annealed in a sequence of increasing temperatures ranging from 400 to 2300 K. After each step the sample is cooled down, and SXPS data are recorded. Sample temperature is measured by a W5%Re-W26%Re thermocouple spot-welded to the side of the W crystal.

III. RESULTS AND DATA ANALYSIS

A. Platinum

1. Film growth and XPS peak shape analysis

An Auger uptake curve for Pt growth on W(211) (Fig. 1) shows distinct breaks occuring at constant intervals. Such behavior is often associated with layer-by-layer growth. Indeed the length of the interval between breaks coincides with the time needed to dose an amount of platinum corresponding to a physical pseudomorphic monolayer as checked by the QCM. [A physical monolayer (ML) is defined, assuming two-dimensional growth, as the minimal coverage at which all substrate atoms are covered by overlayer atoms. In case of W(211) a physical monolayer is 1.63×10^{15} atoms/cm^2.]
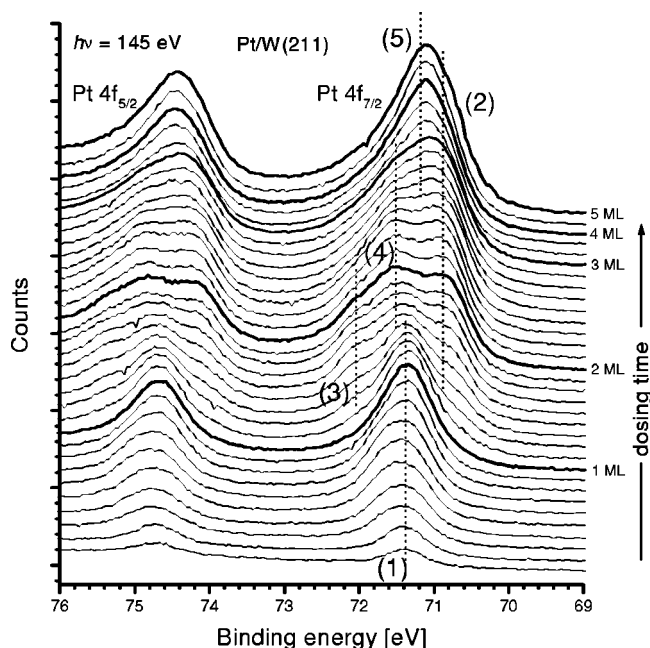
FIG. 2. The Pt $4f$ spectral region recorded during growth of Pt films on W(211) at 300 K.

Pseudomorphic growth of the first two monolayers of Pt on W(211) is also suggested by LEED measurements.[3]

SXPS peak shapes reveal more details about the growth mode. In Fig. 2, a sequence of Pt $4f_{7/2}$ spectra is shown as a function of increasing Pt dose. The growth starts with the formation of the Pt peak denoted by (1) which originates with the Pt monolayer film on W(211). The intensity increases up to the ninth dose, which corresponds to completion of one physical monolayer. For coverages less than one monolayer one can see slight variations in the width of the Pt $4f_{7/2}$ peak which can be attributed to slightly different sites for Pt atoms (the 211 face of the bcc lattice has a row-trough structure) as well as possible adsorbate-adsorbate interactions. Further Pt deposition leads to the formation of clearly visible interesting features—one of them on the low binding energy (BE) side (2), and the other (3) at higher binding energy. Simultaneously peak (1) is attenuated. Peak (2) increases until the second monolayer is completed and it is not attenuated by further Pt deposition. Peak (3) achieves maximum intensity at about 1.7-ML coverage, and then it is gradually attenuated at higher coverages. The peak (4) which is distinct at coverages 1.5–3 ML's is attenuated at higher coverages. Finally peak (5) is formed around 3 ML's and persists during further growth. Based on the order of appearance and attenuation, we tentatively assume that peak (1) is due to monolayer of Pt on W, peak (2) is the surface platinum peak, peaks (3) and (4) are buried interface contributions, and peak (5) is due to bulk platinum. Now the important question is: can we fit these spectra (which show quite a variety of shapes) assuming five different components, and thus support our visual analysis with more quantitative arguments?

Usually x-ray photoelectron spectroscopy (XPS) peaks in metals are properly described by the Doniach-Sunich (DS) (Ref. 10) line shape which accounts for multiple low-energy electron-hole pair excitations at the Fermi level accompanying the core ionization process. However, Pt is a metal with its Fermi level located at the d-band edge and the density of empty electronic states falls rapidly above the Fermi edge. Wertheim[11] suggested that the DS line shape is not appropriate for Pt XPS peak shapes since the DS model contains an implicit assumption that the density of states (DOS) is constant within a few eV around the Fermi energy. An alternative function of the form

$$f(E) = \frac{e^{-E/\xi}}{E^{1-\alpha}} \qquad (3.1)$$

convolved with Gaussian and Lorentzian functions was found to fit the data satisfactorily.[11] In Eq. (3.1) α is the asymmetry (or singularity) index, and in the original DS model, α is proportional to the density of states at the Fermi level of the studied metal; ξ is the parameter describing the electron-hole excitation function to be found from the fit. Binding energy E is measured relative to the line position. The function (3.1) was proposed by Mahan[12] and it accounts for the decreasing DOS above the Fermi level. This function convoluted with a Lorentzian, is equivalent to the DS line shape under the assumption of weakly varying DOS near the Fermi edge (implying large ξ). Our attempts to fit the Pt $4f$ spectra with the function (3.1) have shown that the fit parameter ξ was large compared to the Pt peak width, and the resulting shape does not differ significantly from the DS line shape. Final fits have been made with the DS line shape convoluted with a Gaussian. One has to keep in mind, however, that due to modulation of the DOS close to the Fermi level, the fit parameter α (which measures the DOS at the Fermi level in the original DS model) may not maintain its meaning here. The discrepancy between fitted line shapes from Ref. 11 and from the present work may be attributed to the fact that in Ref. 11 the presence of the surface peak was not taken into account.

We start our analysis from the high coverage side; the two dominant components which are present in the spectrum for the 5-ML film are contributions from bulk platinum and surface platinum. By tilting the sample we are able to change the surface/bulk sensitivity of our spectroscopy and obtain information concerning the location of atoms contributing to the signal (see Fig. 3). The positions and shapes of the spectral components turn out to be identical for both experimental configurations, but relative intensities change considerably. For a 30° grazing take-off configuration we expect less bulk sensitivity, and the peak designated as (5) is found to be less intense. This supports our initial assigment that peak (5) is due to bulk Pt atoms. The centroid of this peak is at 71.1-eV binding energy. All remaining Pt peaks are reported relative to this position. The other peak present for high coverage [peak (2)] shifted by −0.36 eV (to lower binding energy) is assigned to the surface atoms of Pt film. The value of the shift is not far from the literature value of shifts for the Pt(111) surface (0.4 eV);[13–15] however, we do not know details about the surface geometric structure of our 5-ML Pt film. The position of the peak (3), which is shifted by 0.91 eV, is characteristic of a W-Pt alloy (see discussion further in the text) so it is likely that an interface W-Pt alloy is formed upon deposition of a Pt on W substrate. [An ''interface alloy'' component (3) is associated with the situation, when upon adsorption of Pt on W, some number of Pt and W atoms exchange their sites. Analyzing the W $4f$ spectra for
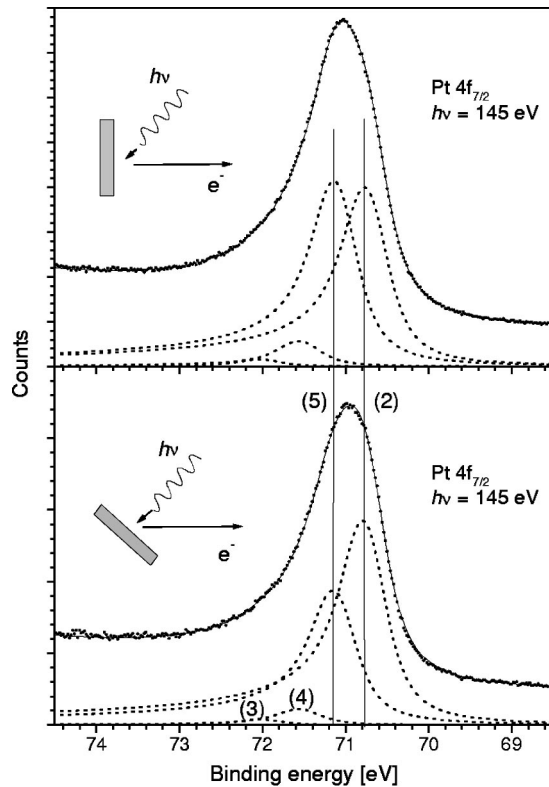
FIG. 3. Pt $4f_{7/2}$ SXPS spectra for 5-ML Pt on W(211), upper: for normal (90°) electron take-off angle, lower: for 30° grazing take-off angle (dotted lines show fitted DS components).

the Pt/W system we found clear evidence that when the Pt coverage is greater than one monolayer, the adsorption of Pt triggers mixing at the interface. This effect is more pronounced for Pt dosed onto the W(111) surface at 300 K and it will be discussed in detail elsewhere[4].]

It has been also found, from the measurements of the attenuation of W peaks as a function of the overlayer thickness (not shown), that the attenuation is exponential and the attenuation length for electrons with energy around 70 eV corresponds to 1.7 pseudomorphic physical monolayers of Pt. The observed intensity ratios for surface/bulk/interface components are all consistent with this attenuation length.

The positions and shape parameters (asymmetry index, the Gaussian width, the Lorentzian width) of all five peaks were determined from spectra in which they constitute the dominant features; then all parameters (apart from amplitudes and background) were kept fixed, assuming that the positions and shapes of photoelectron peaks are dominated by influence of the closest neighbors of the atom being the source of emission. Figure 4 shows the spectra for selected Pt coverages with superimposed fitted line shapes. This, as well as the peak areas as a function of the Pt coverage (discussed below), demonstrate that our assignments allow for consistent interpretation of the obtained data. Figure 5 shows the contributions from different components obtained from the fits of Fig. 4 as a function of dose. The data shown in Figs. 1–5 are all consistent with a layer-by-layer form of growth for Pt on W(211) at 300 K. The positions of all components and singularity indices for the W(211) - Pt adsorbate system, found from the fits, are summarized in Table I.
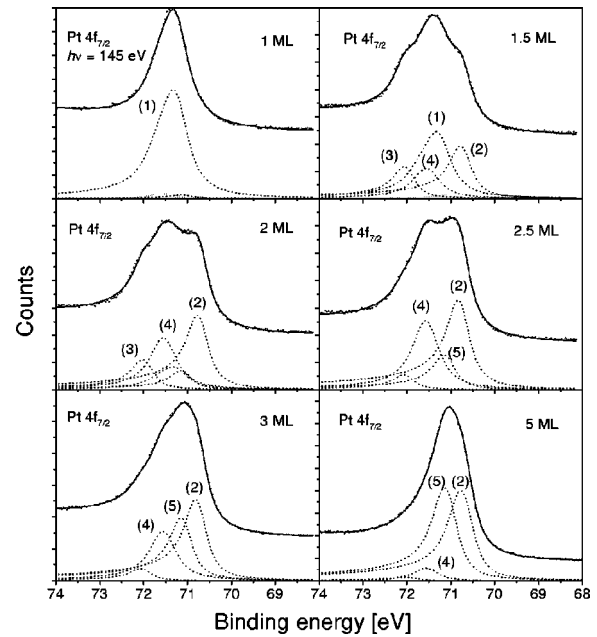
FIG. 4. Doniach-Sunjic (DS) line shape fits to Pt $4f_{7/2}$ data for a few different thicknesses of Pt film on W(211). All parameters describing peak shapes are kept fixed, and only peak amplitudes and background are allowed to change (90° take-off angle).

2. Thermal stability of interface; evidence for Pt/W alloy

An annealing sequence for 1-ML Pt on W(211) is shown in Fig. 6. It can be seen that there is neither change in signal intensity nor change in peak shape for both Pt and W. The stability of the peaks for 1 ML indicates that there is little or no intermixing between Pt and W for this particular coverage.
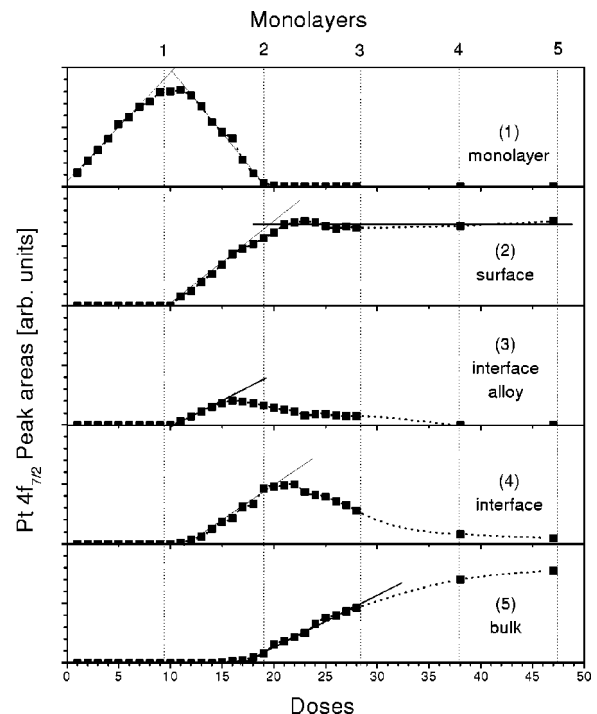
FIG. 5. Areas of DS peaks attributed to various Pt $4f_{7/2}$ spectral components vs Pt film thickness. Arbitrary units are the same for all graphs.

TABLE I. Pt $4f_{7/2}$ peak positions measured with respect to the bulk Pt peak (71.1-eV BE) and singularity indices for the Pt-W system.

Peak	Position (eV)	Singularity index
Bulk	0.00	0.18
Surface	-0.36	0.18
Interface	0.43	0.07
Interface alloy	0.91	0.10
Monolayer	0.17	0.10

For coverages larger than 1 ML, a different behavior is observed (measurements have been made in the range 2–8 ML's and no essential differences in the system properties have been found within this thickness range). It can be seen (see Fig. 7) that the tungsten substrate peak does not change in intensity until the temperature exceeds ~1200 K. This indicates that the platinum deposit on the (211) surface remains flat and does not break into clusters. (If clusters were to form upon annealing, we would expect a significant increase in substrate peak intensity as in the case of Au/W; see Sec. III E.) For the Pt films annealed above 700 K we find a different feature in the W$4f$ SXPS spectra (see Fig. 7). The new peak is shifted by 0.95 eV relative to the bulk W peak. The appearance of this feature is evidence that tungsten atoms diffuse from the interface into the overlayer film to form a platinum—tungsten alloy film. The content of tungsten in the alloy increases with annealing temperature; up to 800 K the tungsten alloy peak remains at constant position and no apparent change is seen in the Pt peak shapes, which indicates that the alloy is dilute. Above 800 K, the W$4f_{7/2}$ alloy
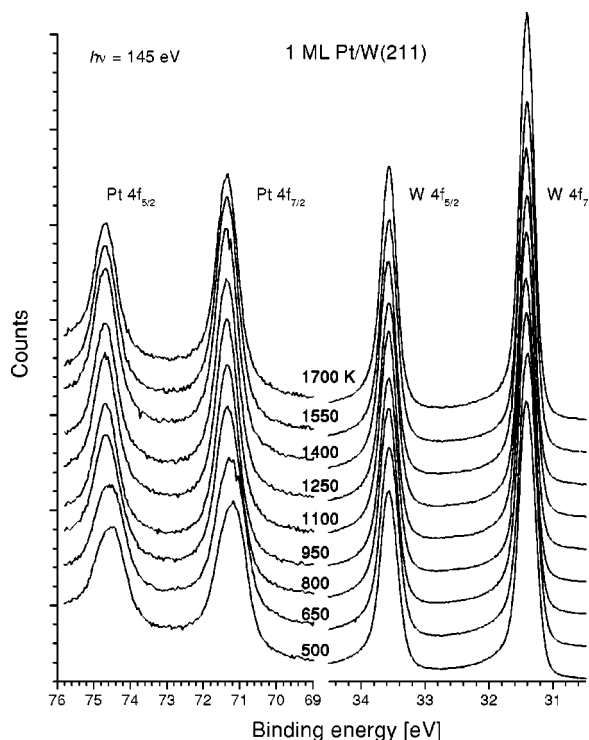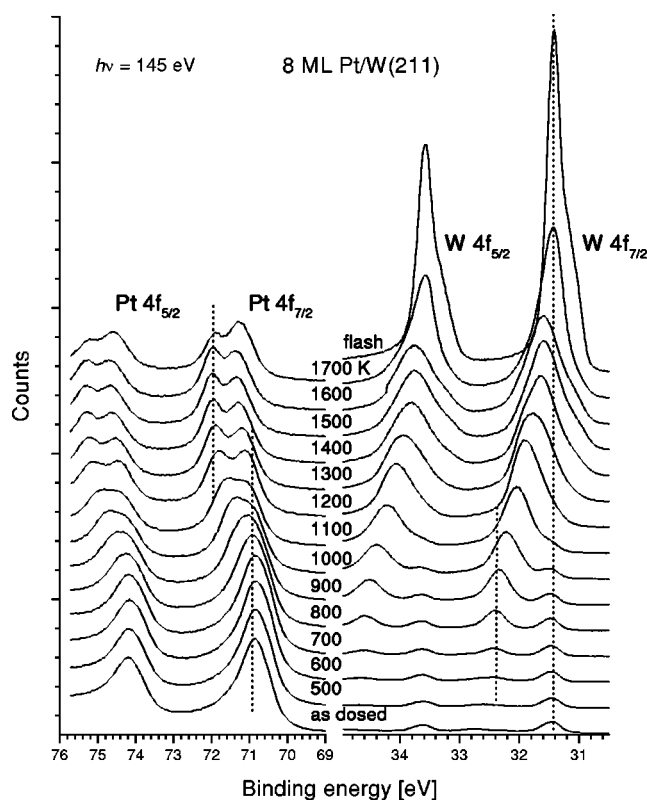
FIG. 7. Pt $4f$ and W $4f$ SXPS spectra associated with annealing sequence for an 8-ML Pt film on W(211). Annealing time is 1 min.

peak in Fig. 7 shifts to lower binding energy and broadens. Simultaneously the platinum peak shifts to higher binding energy and splits into two resolved components. In the temperature range 1400–1600 K the system is stable and no changes in SXPS peak positions and intensities are observed. At 1700 K the onset of Pt desorption is reached[16] which causes a rather dramatic increase in the W $4f$ substrate signal and a decrease in intensity of the higher binding-energy component of the Pt $4f$ peak.

It is expected that a W atom surrounded completely by unlike atoms will experience the maximum core-level shift, while for configurations with both like and unlike nearest-neighbor atoms, the resulting core-level binding energy should be between that of the tungsten bulk and the tungsten impurity in a platinum host. The SXPS peaks shifts and intensity changes, seen in Fig. 7, for annealed Pt/W(211) indicate that initially, the annealing causes a dilute concentration of W in Pt to be formed (which corresponds to maximum W core-level shift); then at 800–1300 K the system goes through a substitutionally random or multiphase configuration (which corresponds to broadening of the peaks). Finally the system reaches a saturated concentration of W in Pt at a temperature of 1400 K which may correspond to ordered intermetallic phase.

The split platinum $4f$ peaks above 1200 K (Fig. 7) evidence a segregation of Pt to the surface. Intensities of these peaks have been measured at different take-off angles (see Fig. 8). Based on the increased surface sensitivity for grazing electron take-off angles we assign the peak at lower BE, shifted by 0.43 eV relative to the Pt $4f$ bulk peak position, to platinum atoms at the sample surface, and the peak at higher BE shifted by 1.19 eV to platinum atoms inside the alloy

FIG. 6. Annealing sequence for a 1-ML Pt film on W(211). The Pt $4f_{7/2}$ and W $4f_{7/2}$ spectral regions are shown following annealing to the indicated temperature for 1 min.
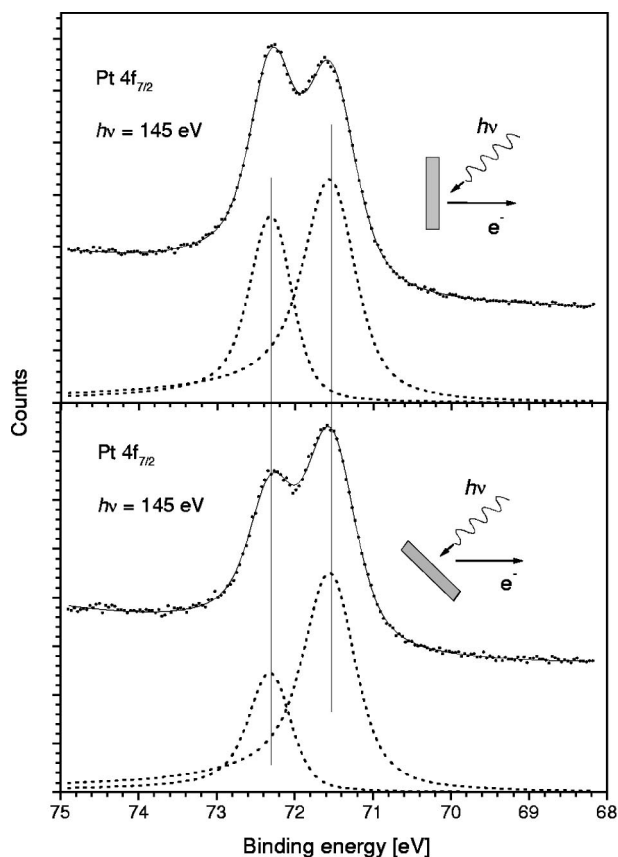
FIG. 8. Pt SXPS spectra of W-Pt saturated alloy. Upper: normal electron take-off angle. Lower: 30° grazing take-off angle. Pt coverage corresponds to ~8 ML's.

film. The Pt $4f$ alloy spectra can be fitted with only two DS components: a broader surface component and a narrower peak from the bulk (see Fig. 8). The intensity of the surface Pt component indicates that the surface is fully covered with Pt. The alloy surface Pt singularity index is found from the fit to be 0.10 and the bulk (alloy) Pt index is found to be 0.09.

B. Palladium

The chemistry of palladium films on tungsten (211) is very similar to that of platinum films. Pd, a $4d$-transition metal, has no narrow photoelectron peaks accessible in our photon energy range, so the data for Pd are limited to W $4f$ photoelectron peaks. In Figs. 9(a) and 9(b) the annealing sequences for 1- and 5-ML films are shown. It is seen that one monolayer of Pd on W(211) is stable; no change in intensity or in peak shape occurs below the desorption threshold around 1300 K (no evidence for intermixing or surface alloy formation). Annealing above 1300 K uncovers the tungsten surface [this is indicated by surface W peaks appearing in the SXPS spectra; see Fig. 9(a)]. A more detailed discussion of the relation between W $4f$ surface core level shifts and the W(211) surface structure can be found in Refs. 3 and 18. For the 5-ML Pd film one can observe virtually the same features as for Pt films; a dilute alloy up to 850 K, and increasing W content in the film at higher temperatures. Around 1100 K the alloy saturation is accompanied by the onset of Pd desorption which causes a rapid
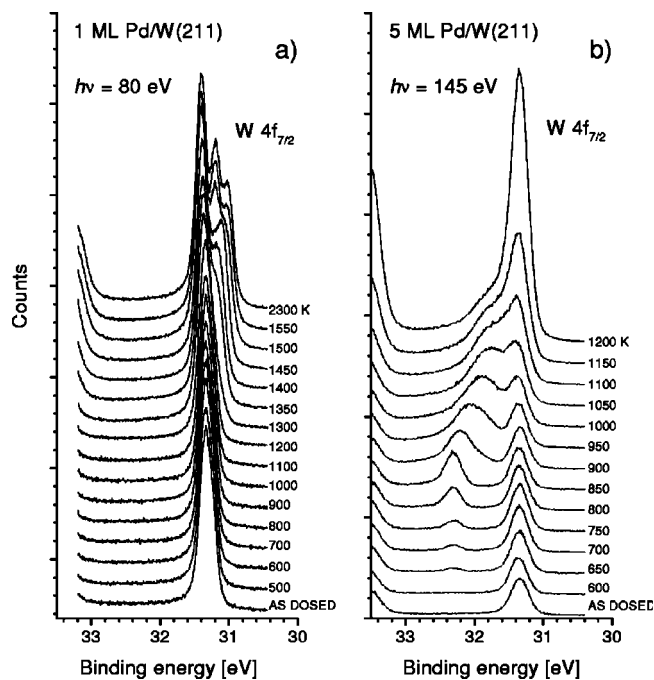
FIG. 9. W $4f_{7/2}$ SXPS spectra associated with Pd/W(211): (a) annealing sequence for a 1-ML Pd film on W(211), (b) annealing sequence for a 5-ML Pd film on W(211).

increase in intensity of the substrate W peak. [For 5–8-ML films a higher photon energy, 145 eV, has been used in order to probe a few monolayers inside the bulk of the film. Spectra taken with these higher photon energies have significantly worse resolution (and intensities), i.e., the distinct surface W peaks of Fig. 9 appear as much weaker shoulders, in Fig. 7.]

C. Iridium

The Ir $4f$ SXPS spectra for increasing Ir coverage on W(211) are shown in Fig. 10. A very interesting property of
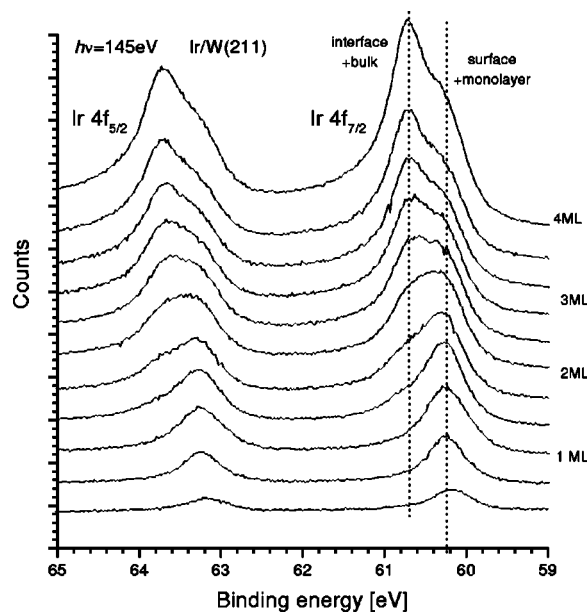
FIG. 10. Ir $4f$ spectral region recorded during growth of Ir film on W(211) at 300 K.
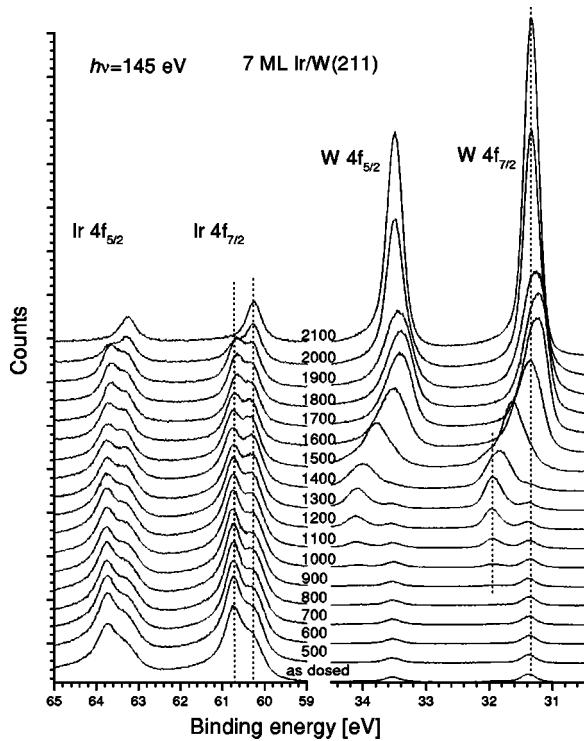
FIG. 11. Ir $4f$ and W $4f$ SXPS spectra associated with anneal-ing sequence for a 7-ML Ir film on W(211). Annealing time is 1 min.

FIG. 12. W $4f_{7/2}$ SXPS spectra associated with: (a) annealing sequence for a 1-ML Rh film on W(211), (b) annealing sequence for an ~8-ML Rh film on W(211).

iridium is that the initial peak (which is attributed to cover-age of a single monolayer) and the Ir surface peak on a thick Ir film (the assigment of the latter has been checked by mea-surements at different take-off angles), are isoenergetic. Moreover, no separate interface feature is seen. The spectra may be fitted with two Doniach-Sunjic components at a binding energy of 60.80 eV (interface+bulk) and a binding energy of 60.25 eV (surface+single monolayer). This, as well as the annealing experiment (see Fig. 11) demonstrate that the Ir $4f$ binding energies are not changed if the neigh-bor Ir atoms are replaced by W atoms. This is quite different from the spectra seen for Pt (Fig. 2). On the other hand, Fig. 11 demonstrates that the Ir-W system is in some ways very similar to Pt-W. The dilute alloy features are observed in the annealing temperature range 1000–1400 K; at higher tem-peratures the alloy W peaks broaden and shift to lower bind-ing energy until the saturated alloy phase, reflected by stable SXPS spectra within the range 1800–2000 K, is reached. At about 2100 K, the desorption threshold for multilayer iridium causes an increase in the substrate W peak intensity. The iridium peaks do not change positions significantly during the annealing experiment, and the intensity of the surface peak is stable within the whole temperature range, reflecting the fact that the outer layer is always pure iridium. The main Ir peak (which may contain up to three contributions—the interface, the Ir metal bulk, and the W-Ir alloy bulk) de-creases upon alloy formation, reflecting a decreased content of Ir in the film. The asymmetry index of the $4f_{7/2}$ features for a pure Ir film is 0.14 and that of the Ir line from the saturated alloy is 0.06. Above 2100 K, the bulk Ir peak dis-appears and only a single monolayer of Ir on tungsten is left.
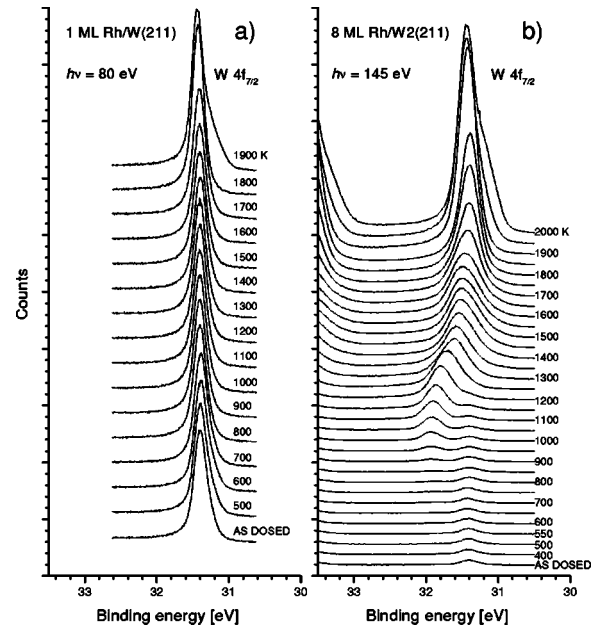
D. Rhodium

The phenomena associated with annealing of Rh films on W(211) are similar to the cases of Pt, Pd, and Ir films dis-cussed above. As Rh is a 4d metal, the data are limited to the SXPS spectra of the W $4f$ region (see explanation in Sec. III B). Annealing sequences for a single monolayer film and for a film approximately eight monolayers thick are shown in Figs. 12(a) and 12(b). For a single Rh monolayer annealed to temperatures below the desorption threshold, the shape and intensity of the W $4f_{7/2}$ peak do not change. This indicates that a physical monolayer of Rh on W(211) is stable over a broad temperature range. Above 1800 K, the Rh film is de-sorbed and the shoulder on the low-binding-energy side of the W peak corresponding to surface tungsten atoms is re-vealed [Fig. 12(a)]. For the multilayer film, a dilute alloy peak is observed within the temperature range 850–1100 K. A saturated (stable) alloy phase exists between annealing temperatures of 1400–1600 K [see Fig. 12(b)].

E. Gold

A sequence of SXPS spectra for increasing Au coverage on the W(211) substrate is presented in Fig. 13. Au has a low density of states at the Fermi level and asymmetries of the SXPS peaks are very small. The spectra have been fitted with DS line shapes and the analysis that we perform is similar to the Pt analysis described in Sec. III A. In the submonolayer range there is significant variation of the SXPS peak posi-tion. This behavior is most probably caused by complex ini-tial stages of growth as discussed by Kolaczkiewicz and Bauer in Ref. 17. After one monolayer [peak (1)] is com-pleted, the peak attributed to Au surface atoms [peak (2)], and the peak attributed to Au interface atoms [peak (3)] ap-pear. Within the 2–3-ML range, the spectra are dominated by the surface peak and above 3 ML's the bulk peak (4) becomes clearly visible. The DS peak areas are shown in Fig.
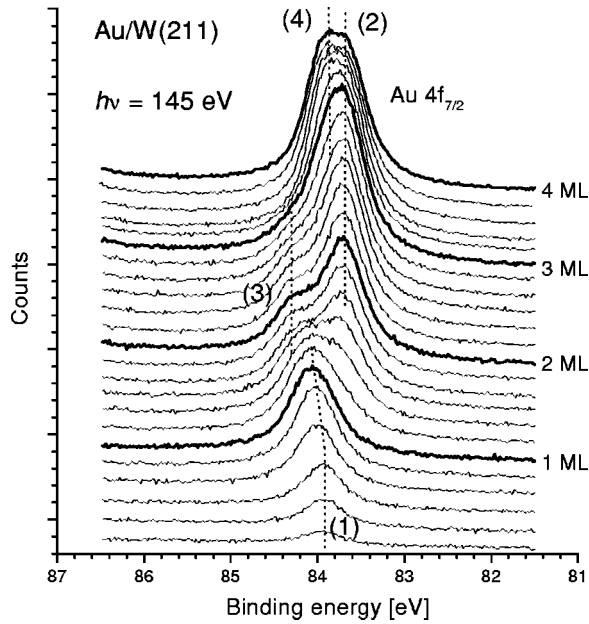
FIG. 13. Au $4f_{7/2}$ spectral region recorded during growth of Au films on W(211) at 300 K.
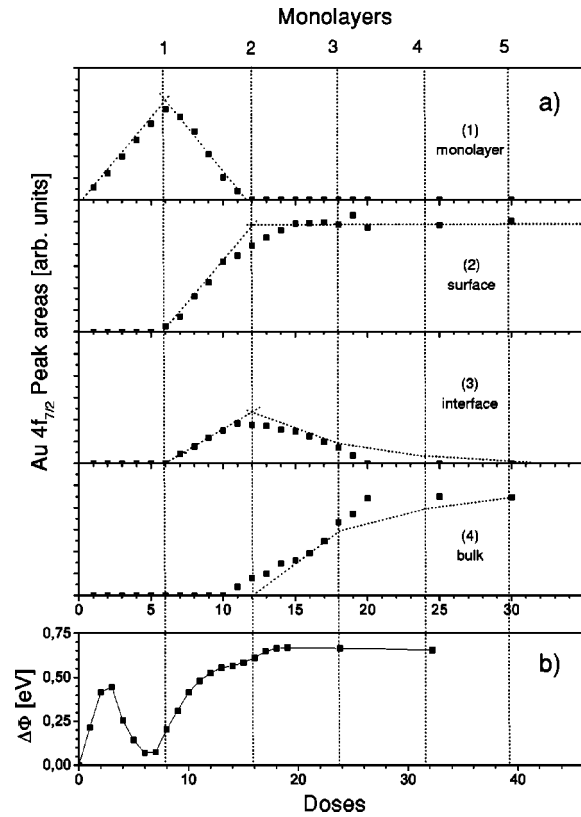
FIG. 14. (a) Areas of Au $4f_{7/2}$ (DS) Au peaks attributted to various spectral components vs Au film thickness. Arbitrary units are the same for different part of the figure. (b) Work function change associated with Au film growth on W(211). The dose time and the Au deposition rate are different for experiment (a) and (b) but the graphs are recalibrated to make the coverage scale common. Dotted lines are drawn to show the peak areas expected for a layer-by-layer growth.

TABLE II. Au $4f_{7/2}$ peak positions measured with respect to bulk Au peak (83.9-eV BE).

Peak	Position (eV)
Bulk	0.00
Surface	− 0.32
Interface	0.36
Monolayer	0.01

14(a). It can be seen that the film formation is basically a form of layer growth. The work function change has been monitored during Au film growth (by measuring the low-energy cutoff for photoelectron emission) and compared with work function data reported by Kolaczkiewicz and Bauer[17] for Au growth on W(211); see Fig. 14(b). The assignment of one pseudomorphic physical monolayer coverage is consistent in both experiments. SXPS peaks positions for adsorption of Au on W are summarized in Table II.

During an annealing experiment, the processes observed for Au on W(211) are distinctly different from processes observed for Pt, Pd, Ir, and Rh. A ∼6 ML gold film is stable against thermally activated rearrangement up to 500 K, as indicated by Fig. 15. Above this temperature the substrate signal rises substantially and this rise is accompanied in the Au $4f$ region by a reduction of the main peak intensity and the appearance of an additional peak characteristic of single-monolayer Au/W film. Above 750 K, the spectra do not change until 1200 K, where the thermal desorption threshold for multilayer Au is reached. This behavior is characteristic of clustering of the gold deposit in excess of one physical monolayer for $T > 500$ K.

F. Valence-band spectra

The valence-band spectra of pure Pt, Pd, Ir films have been compared with the valence spectra of saturated alloys
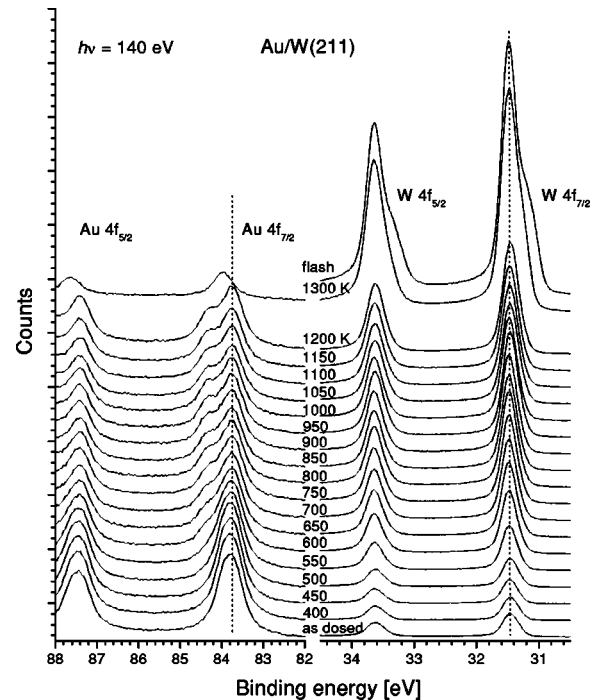
FIG. 15. Au $4f$ and W $4f$ SXPS spectra associated with annealing sequence for a 6-ML Au film on W(211).
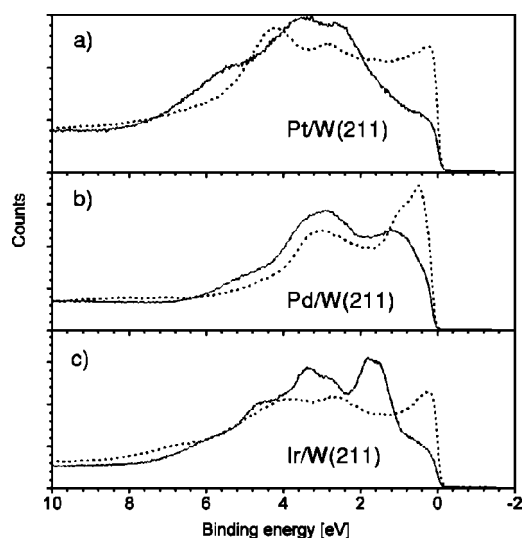
FIG. 16. Valence-band spectra of pure thick (~5 ML) metal films (dashed lines) and saturated alloys of these metals with tungsten (solid lines). (a): Pt/W(211); (b): Pd/W(211); (c): Ir/W(211).

of these elements with tungsten [see Figs. 16(a)-(c)]. All three systems show common behavior; upon alloying the photoelectron signal at the Fermi level decreases and the center of the band shifts to higher binding energy. Due to the fact that the number of valence electrons and the cross section for ionization increases from left to right across the "d" row in the periodic table,[19] it is believed that the alloy spectra are dominated by signal from the late transition metal. For the photon energies used in the present experiment, the measured valence-band curves should resemble the total density of states. The reason for this is that the final states for photoelectrons of energies above 30 eV can be approximated by continuum states and the strict one-electron momentum conservation requirement is removed by many-body relaxation effects.[20] The changes of the valence-band spectral character have been investigated over a broad range of observation angles, and both the decrease of intensity at the Fermi level and the spectral shift has been always observed. Thus these changes are believed to arise from changes in the total density of states. These findings are consistent with the fact that the asymmetry (α) of Ir and Pt SXPS lines decreases upon alloy formation (see Table III).

G. Surface structure

LEED studies have been performed for single- and multilayer films of Pt, Ir, and Rh on W(211). It has been found that the "as dosed" films have the 1×1 pseudomorphic structure. The diffuse LEED spots indicate poor order for "as dosed" 4–8-ML films. However, "diluted" and

TABLE III. Comparison of asymetry indices of the Doniach-Sunich lines from late transition metals and from their tungsten based alloys.

Atom	Pure metal film	Alloy film
Pt	0.18	0.09
Ir	0.14	0.06

"saturated" alloy films both have distinct pseudomorphic geometrical order. The images show well defined surface periodicity along the $\langle 1\bar{1}\bar{1}\rangle$, and streaky spots along the $\langle 0\bar{1}1\rangle$ direction [across the rows and troughs of the W(211) surface] suggest distortion of the crystallographic order along this direction.

IV. DISCUSSION

A. Film growth

Experimental data concerning the growth of the late transition metals on the W(211) plane are scarce in the literature. In fact, with the exception of Au and Ni on W(211) reported in Ref. 17, and the earlier paper of the present authors[3] concerning Pd and Pt growth on W(211), there have been no published papers on this topic. However, the growth of late transition metals has been extensively studied on W(110).[21–25] In Ref. 17 it was shown that the initial stage of growth for Au on W(211) is very complex. At room temperature the adatoms on the W(211) surface have enough mobility to align initially in long chains along rows in the $\langle \bar{1}11\rangle$ substrate direction.[26] For coverages below 0.5 physical monolayer, LEED images are interpreted to indicate the formation of long pseudomorphic Au rows in substrate troughs; unoccupied troughs are left between Au rows. This phase of growth may correspond to the lowest three spectra in Fig. 13. For multilayer coverages, LEED and Auger data suggested the formation of an Au(111)-like film, but many transition phases were observed for intermediate coverages. Because the atomic radii of Pt, Pd, Au, Ir, Rh, and W do not differ significantly, the deposited atoms tend to form pseudomorphic overlayers initially. LEED studies of the growth of Pt and Pd on W(211) at room temperature have shown that the initial layers are indeed pseudomorphic.[3] As suggested by diffuse and streaky LEED images,[16] "as dosed" layers are distorted for coverages greater than 2 ML's. (Annealing or deposition at elevated temperatures has been suggested in Ref. 22 to improve the film order, but it is very likely that an alloy film is formed in this way.) On W(110), the growth was found to be a layer-by-layer type over a broad (>20 ML's) thickness range (see for example Refs. 24 and 25). The "flat" growth is found also on W(211) for all admetals studied in the present experiment over a broad coverage range (1–8 ML's); this is based on the observation that the height of the substrate W $4f_{7/2}$ peaks is found to decrease exponentially with the overlayer thickness. The SXPS line shapes strongly indicate the layer form of growth in the range 1–3 ML's.

B. Monolayer films vs multilayer films: thermal stability

In all cases a monolayer of deposited Pt, Pd, Ir, Rh, Au is stable on W(211). This is consistent with previous results obtained by low-energy ion scattering[27] and Auger electron spectroscopy.[16] This stability is attributed to surface energy minimization when the monolayer deposit stays flat on the tungsten substrate.[1,28] LEED studies[16] indicate that the annealed single monolayer films are highly ordered and pseudomorphic. In contrast, when a multilayer deposit of Pt, Pd, Ir, or Rh is annealed (above 700 K for Pt and Pd, and above 900 K for Ir and Rh), tungsten atoms diffuse into the

overlayer film to form an alloy. A dilute alloy phase is observed below 900 K for Pt and Pd and below 1300 K for Ir and Rh. Heating to temperatures higher than ones listed above rapidly increases the content of tungsten in the film; this is accompanied by broadening and shifting of W $4f$ photoelectron peaks caused by formation of a substitutionally random alloy or the coexistence of different alloy phases. For Pt, Ir, Rh the saturated alloy phase is seen over broad annealing temperature ranges (~ 200 K; heating in these ranges does not modify the alloy film composition and structure as indicated by stability of SXPS peaks shapes and amplitudes). As indicated by Pt $4f_{7/2}$ and Ir $4f_{7/2}$ spectra (see Fig. 8) the top layer of investigated alloys is composed of the segregated late transition metal atoms (Pt or Ir). In general the alloying behavior of investigated bimetallic samples is consistent with known bulk phase diagrams.[29,30] The W-Pt alloy phase diagram indicates a very limited solubility of Pt in a W matrix; however, the diffusion of W into Pt is possible up to a maximum content of ~ 60 at. % tungsten. The phase diagram for the W-Pd system is similar to that of W-Pt but the limiting concentration of W in Pd is only 21 at. %. Also for W-Ir and W-Rh the phase diagrams show marginal solubility of Ir and Rh in a W host and substantial solubility of W in Ir or Rh hosts. Au and W are not known to form chemical compounds. For Pt, Ir, and Rh the alloy phase diagrams[29,30] show the existence of a few ordered phases and it is possible that these phases are formed during annealing of our films. However, we cannot exclude the possibility that for the ultrathin alloy films studied here, the presence of the interface and the segregated surface layer may force a structure different from known bulk phases.

C. Chemical shifts of photoelectron peaks

In the simplest view, the *charge transfer* onto or off an atomic site in a crystal causes a shift in the core-electron binding energy. Although this mechanism may dominate in cases where the charge transfer is substantial (i.e., ionic compounds), for metals and alloys there are several other factors which have to be taken into account. These include rehybridization of valence orbitals, changes in final-state screening, Madelung potential terms, and reference level shifts.[7] We briefly discuss these effects for transition metals and alloys below.

Covalent bonding (intra-atomic charge transfer, rehybridization). Transition metals have two types of chemically active electrons: d and sp like. Alloying of transition metals involves an interplay between d and s,p band effects. Late transition elements often lose d-like electrons when alloyed with early transition elements; the d orbitals of the alloy constituents hybridize and the hole character of the partially filled d orbitals of the early element mix into the nearly fully occupied d orbitals of the late element.[31] The change of a localized d charge on an atomic site is usually compensated by the opposite flow of free s,p-like charge.[32] This phenomenon is often addressed as sp-d compensation. In atoms of the $5d$ row (Pt, Ir, W), the $6s,p$-$6d$ orbital filling changes have a twofold effect on the energy of the $4f$ level. First, a part of the screening of the nuclear charge provided by the inner d-like electron density is removed. Second, the inner $5d$ and $4f$ electron densities significantly overlap and this

overlap is also partially removed. Both of these effects tend to increase the binding energy of electrons in the $4f$ level (see, for example, the radial electron distributions in Ref. 33).

Changes in final state screening. The core-ionization process in metals and alloys is usually considered within the complete screening model in which the metallic electronic structure relaxes completely to the ground state of the core hole-metal system. There is no general solution to the problem of how much the screening influences SXPS line positions when the metallic environment of the source atom is changed. In the case of Au (Ref. 34) the relaxation energy term was found to be ~ 17.7 eV and the major contribution to it was from the charge rearrangement localized on a single site (17.1 eV). 90% of the remaining 0.6 eV was attributed to screening by the nearest neighbors. As the screening in transition metals depends on the charge-density character (d or s,p) (Ref. 35) it is expected that whenever the local configuration changes (i.e., as a result of alloying) the screening contributions to the SXPS line position change as well. However, the studied metals have high density of states at the Fermi level and it is believed that differential final-state effects are reasonably small. For example, for surface Ta atoms on Ta(100), it has been demonstrated[36] that the differential final-state effect was only 0.1 eV. In the present experiments observed SXPS line shifts are of the order of 0.3–1 eV and we assume the final-state effects are merely corrections and do not dominate the line shifts.

Madelung potential terms. For the bimetallic systems studied here, the interatomic charge transfer tends to be small due to the s,p-d compensation mechanism. In such a case there is no ''ionic network'' which could add a Madelung-type term to the electrostatic potential experienced by core electrons. Therefore the ''Madelung'' shifts of SXPS lines should be insignificant.

Reference level shift. In the case of metallic samples, only the value of $\Delta(\epsilon_{4f} - \epsilon_F)$ can be obtained experimentally (where ϵ_F and ϵ_{4f} are the Fermi edge and $4f$ level energies). However, if one hopes to refer the measured core-level energy shifts in the alloy to the initial-state chemistry, he must use the value of $\Delta\epsilon_{4f}$ as it reflects (in the case when final-state effects are small) the chemical effects. Unfortunately, there is no experimental method for relating the vacuum level and the Fermi level in the case of transition metals and their alloys, since the dominant contribution to the work function is the surface dipole.[6] Moreover, in the alloy systems under investigation, the surface is covered by the segregated late transition metal. In this way the change in $\Delta\epsilon_F$ upon alloying may mask the ''true'' core-level shift.

The electronegativities of Pt (2.3), Pd (2.2), Ir (2.2), and W (1.7) might suggest that electron transfer from W to Pt (Pd, Ir) is likely. However, upon alloying, in the case of Pt, both Pt and W $4f$ peaks are shifted the same direction (to higher binding energy) and in the case of Ir on W(211), the W $4f$ peak shift direction depends on concentration of W in Ir (it shifts to higher binding energy for the dilute alloy and to lower binding energy for the saturated alloy) and the Ir $4f$ peaks do not exhibit significant shifts at all. These observations as well as the earlier discussion indicate that the core-level shifts observed upon transition-metal alloying are not dominated by interatomic charge transfer. The two additional

factors which have to be taken into account are s,p-d intra-atomic charge transfer and the Fermi-level shift (with reference to the core levels). Watson, Davenport, and Weinert[37] calculated the core-level shifts (referred to ϵ_F) for a number of ordered transition alloys (1:1 composition) having the CsCl structure with a self-consistent local density-functional model. For a Pt-W alloy, the shifts are indeed in the same direction; to higher binding energy, and are ~ 0.5 eV for Pt and ~ 0.6 eV for W. Assuming that the W peak area is proportional to the W concentration in the alloy and that the limiting concentration of W in Pt is 60 at. %, we can estimate the W concentration in the alloy and find the set of data close to 1:1 composition. It turns out that the film annealed to 1200 K is close to the 1:1 composition. For this film we have experimental shifts of ~ 0.8 eV for Pt and ~ 0.5 eV for W. They are in qualitative agreement with calculated values. As shown in calculations[37] these shifts arise mainly from the ϵ_F change and have no transparent relationship to the alloy chemistry.

Iridium does not exibit significant peak shifts when it is in contact with tungsten. The reason may be that both ϵ_F and ϵ_{4f} shift in parallel, or both do not shift at all. In fact, it is often found when alloying two metals, that both the Fermi level and the core-level shift by comparable amounts.[6] This is a consequence of simple electrostatics; if a negative charge is added to an atom as a result of difference in chemical potential (assuming a spherical excess charge residing outside the ''atom''), both the valence-electron levels and the core-electron levels shift by the same amount with respect to the vacuum level. No change in the core-level position is seen then with respect to the Fermi level. The stability of Ir peaks is most probably associated with such a situation. The negative charge is added to s and p orbitals but the d orbital occupancy is not changed. There are no complex rehybridization processes occuring on iridium atoms which approach contact with tungsten atoms upon alloying or adsorption on a W surface. No significant changes in final state screening are anticipated either, since final-state screening is dominated by ''on site'' screening. This enables us to understand the puzzle of how so many contributing effects may cancel together to produce a zero shift irrespective of whether an Ir atom exists in a monolayer film adsorbed on a W surface or in an alloy of any concentration. On the other hand, the complicated behavior of the W $4f$ peaks suggests that the interplay of charge transfer, rehybridization, final-state, and reference-level effects occur on the W atom approaching contact with Ir.

Both the magnitudes of the diluted-alloy tungsten peak shifts and the temperatures at which the tungsten atoms diffuse into the deposited metal films are very similar in pairs composed of neighboring elements in the same columns of the periodic table: Pt/W-Pd/W and Ir/W-Rh/W. This suggests strongly that the basic chemistry is very similar in these pairs.

D. Thermochemical data from XPS shifts

A relatively simple alternative to the difficult analysis of XPS peak positions in terms of the initial core levels/final-state effects is provided by a Born-Haber cycle together with the equivalent core approximation (ECA). For example the

TABLE IV. Comparison of surface peak shifts with the segregation energies from Ref. 39.

Host (impurity)	Surf. XPS shift (eV)	Segr. energy (eV)
Pt (Au)	-0.36	-0.32
Ir (Pt)	-0.50	-0.57
Au (Hg)	-0.31	

segregation energy of a Au impurity in Pt to the Pt/W interface should be equal to the interface Pt shift (0.43 eV) and the segregation energy for a gold impurity in a Pt host to the Pt surface should be equal to the surface Pt peak shift (-0.36 eV).[38] The difference between the positions of surface and interface peaks (-0.80 eV) should be, in this scheme, equal to the difference between the adhesion energies per atom of Au and Pt on the W(211) surface. Heats of surface segregation for a number of transition-metal impurity atoms in transition-metal hosts have been calculated recently in a density-functional framework by Christensen et al.[39] A comparison of the values extracted from our data with this calculation is shown in Table IV. Satisfactory agreement is found.

The shift of a dilute W peak (ΔE) may be related by a Born-Haber cycle and the ECA to an expression containing solution energies for certain metallic systems.[40] For the dilute alloys studied in this work we have

$$\Delta E_{W/Pt} = E_{(W;Pt)} + E_{(Re;W)} - E_{(Re;Pt)}, \qquad (4.1)$$

$$\Delta E_{W/Pd} = E_{(W;Pd)} + E_{(Re;W)} - E_{(Re;Pd)}, \qquad (4.2)$$

$$\Delta E_{W/Ir} = E_{(W;Ir)} + E_{(Re;W)} - E_{(Re;Ir)}, \qquad (4.3)$$

$$\Delta E_{W/Rh} = E_{(W;Rh)} + E_{(Re;W)} - E_{(Re;Rh)}, \qquad (4.4)$$

where $E_{(A;B)}$ is the solution energy of metal A in metal B. No experimental information on required solution energies has been found. The heats of solution have been then calculated according to Miedema's[41] semiempirical scheme. The comparison of our shifts with shifts derived from Miedema's solution energies is presented in Table V. Unfortunately, although a strong correlation between Miedema's estimates and the experimental solution energies exists,[40] the estimates have rather large error. Since expressions (4.1)–(4.4) contain three such terms, relative errors may be multiplied. As is seen from the table the sign of the shift is predicted correctly for all four systems, but the obtained values of the shifts do not reflect even the trends (Rh and Ir shifts are significantly smaller than Pt or Pd shifts). Thus the coincidence of Miediema's estimate and the measured dilute alloy shift for Pd is most probably accidental.

TABLE V. XPS peak shifts in dilute alloys.

Host (impurity)	Measured shift (eV)	Miedema est. (eV)
Pt (W)	0.95	1.22
Pd (W)	1.00	1.04
Ir (W)	0.50	1.03
Rh (W)	0.50	0.90

There may be uncertainties in the above comparison, arising from the application of the ECA to the shallow core levels used in this work. The ECA is general for any core level and the assumption has to be made that the shifts are equal for all core levels in an atom. Intra-atomic charge transfer/rehybridization energy terms (which can arise from the $5d$ and $4f$ overlap in $5d$ atoms) may be specific to the $4f$ levels, but they may not be applicable to deep core levels. (Because of the available photon energy range we have not tested the values of shifts for core levels other than $4f$; in any event the deeper core-level XPS peaks tend to be broad and precise determination of their shifts may not be possible.)

E. Valence-band restructuring upon alloying

Effects of chemical bonding are reflected in the valence-band density of states and consequently in photoelectron valence-band spectra. The late transition-metal electronic structure is characterized by a system of narrow d-like bands and broad s,p-like bands.[42] A high DOS at the Fermi level for late transition metals is due to d-like electrons. The overall character of changes which occur in valence-band spectra due to alloying is common for all the systems studied (W-Pt, W-Pd, and W-Ir); alloying causes a lowering of the density of states at the Fermi level and a shift of the center of the band to higher binding energy. Similar behavior was observed by Bzowski and Sham for the $PdTi_2$ ordered alloy.[43] The depletion of DOS intensity at the Fermi level and the shift of the center of the valence band to higher binding energy seem to be universal behavior when the late transition metal is alloyed with a more ''electropositive'' element.[19] It has been argued that this is due to filling of d bands of the late transition metal so the d band is no longer pinned to the Fermi level but adjusts its position to minimize system energy (thus the valence band is becoming gold like).[19,44] However, the experimental work by Bzowski and Sham[43] based on the intensity of the so-called x-ray absorption near-edge structure ''white line'' in the $PdTi_2$ intermetallic sample has shown that the d band of Pd is depleted, not filled upon alloy formation. (Nevertheless, the valence band showed the same behavior, narrowing and shifting away from the Fermi level.) Fernando, Watson, and Weinert[45] noticed that the d-band filling in the PtTi compounds (where the basic chemistry should be very similar to PdTi) is not associated with Ti electrons transferring into the empty Pt levels but rather there is a reduction in the overall Pt d count due to hybridization of Ti wave-function character into the Pt subband. Pan, Ruckmann, and Strongin[46,47] also argued that in Pt/Nb and Pd/Ta alloys the changes in the d band count (and the changes of the valence-band spectra) occur due to rehybridization of d bands rather than due to configuration changes. Moreover, calculations in Ref. 48 show that there is signifi-

cant non-d character hybridized into the occupied d bands of the elemental metals. Thus a mix of different factors is at play; a charge transfer in the usual sense, involving filling or emptying of individual bands, as well as hybridization and screening from both d and non-d electrons. A simpler picture based on extended molecular orbitals rather than an atomic approach to understand these results was proposed by Strongin *et al.* in Ref. 49. The changes of density of states at the Fermi level in this picture have been related to redistribution of electrons on bonding and antibonding states upon alloying.

V. CONCLUSIONS

Several late transition metals (Pt, Pd, Ir, Rh, Au) grow in layers on W(211). For the initial few monolayers the films are pseudomorphic. A single monolayer of these metals on W(211) is stable against thermally activated rearrangement, which is attributed to a surface free-energy minimum for this configuration. For multilayers of Pt, Pd, Ir, Rh heated to 700–1000 K, substrate atoms diffuse into the overlayer to form a dilute alloy. Further heating leads to formation of saturated alloy phases. The outermost layer of these alloys is composed of segregated late transition metal. The alloys preserve the geometrical structure of the substrate and remain flat upon annealing; there is no evidence for clustering of the overlayer metal in excess of one physical ML. In contrast gold films do not form alloys; moreover the overlayer material in excess of one physical monolayer is converted into three-dimensional clusters upon heating. In one case [Pt on W(211)] a limited amount of adsorption-triggered interfacial mixing is observed upon deposition of multilayers at 300 K; such interfacial mixing is not observed for deposition of Pd, Rh, Ir on W(211) at 300 K. SXPS peak shifts are caused by an interplay of many competing effects and no transparent relationship with alloy chemistry is found. Photoelectron peak shifts observed on late-transition-metal surfaces, analyzed according to the Born-Haber/ECA scheme, are consistent with recent calculations[39] of segregation energies. No satisfactory agreement is found, however, between the SXPS shifts in dilute alloys and solution energies calculated according to Miedema's semiempirical scheme. Valence bands of alloys show a decreased density of states at the Fermi level and shifts of their centroid to higher binding energy (compared to pure late-transition-metal spectra); this is an effect of bond formation between tungsten and late-transition-metal atoms.

*Present address: Instytut Fizyki, Uniwersytet Jagielloński, Reymonta 4, 30-059 Krakow, Poland.

†Corresponding author. Email: madey@physics.rutgers.edu

[1] T.E. Madey, J. Guan, C.-H. Nien, C.-Z. Dong, H.-S. Tao, and R.A. Campbell, Surf. Rev. Lett. **3**, 1315 (1996).

[2] T.E. Madey, C.-H. Nien, K. Pelhos, J. Kolodziej, I. Abdelrehim, and H.-S. Tao, Surf. Sci. **438**, 191 (1999).

[3] J.J. Kolodziej, K. Pelhos, I.M. Abdelrehim, J.W. Keister, J.E. Rowe, and T.E. Madey, Prog. Surf. Sci. **59**, 117 (1999).

[4] J.J. Kolodziej, J.W Keister, J.E Rowe, and T.E. Madey (unpublished).

[5] J.A. Rodriguez, Surf. Sci. Rep. **24**, 223 (1996).

[6] W.F. Egelhoff, Jr., Surf. Sci. Rep. **6**, 253 (1987).

[7] R.E. Watson and M.L. Perlman, Phys. Scr. **21**, 527 (1980).

[8] B. Johansson, N. Martensson, and C. Jones, Phys. Rev. B **21**, 4427 (1980).

[9] P. Steiner and S. Hufner, Acta Metall. **29**, 1885 (1981).

[10] S. Doniach and M. Sunjic, J. Phys. C **3**, 285 (1970).

[11] G.K. Wertheim and L.R. Walker, J. Phys. F: Met. Phys. **6**, 2297 (1976).

[12] G.D. Mahan, Phys. Rev. B **11**, 4814 (1975).

[13] R.C. Baetzold, G. Apai, and E. Shustorovich, Phys. Rev. B **26**, 4022 (1982).

[14] G. Apai, R.C. Baetzold, and E. Shustorovich. Surf. Sci. **116**, L191 (1982).

[15] M.L. Shek, P.L. Stefan, C. Binns, I. Lindau, and W.E. Spicer, Surf. Sci. **115**, L81 (1982).

[16] K. Pelhos, I.M. Abdelrehim, C.-H. Nien, and T.E. Madey, J. Phys. Chem. (submitted).

[17] J. Kolaczkiewicz and E. Bauer, Surf. Sci. **144**, 477 (1984).

[18] H.-S. Tao, J.E. Rowe, and T.E. Madey (unpublished).

[19] J.C. Fuggle, F.U. Hillebrecht, Z. Zolnierek, P.A. Bennett, and Ch Freiburg, Phys. Rev. B **27**, 2145 (1982).

[20] N.V. Smith, G.K. Wertheim, and M.M. Traum, Phys. Rev. B **10**, 3197 (1974).

[21] J.A. Rodriguez, Surf. Sci. **345**, 347 (1996).

[22] J. Kolaczkiewicz and E. Bauer, Surf. Sci. **314**, 221 (1994).

[23] S.M. Shivaprasad, R.A. Demmin, and T.E. Madey, Thin Solid Films **163**, 393 (1988).

[24] H. Wormeester, E. Huger, and E. Bauer, Phys. Rev. B **57**, 10 120 (1998).

[25] H. Wormeester, E. Huger, and E. Bauer, Phys. Rev. B **54**, 17 108 (1996).

[26] S.C. Wang and G. Ehrlich, Surf. Sci. **206**, 451 (1988).

[27] C.Z. Dong, L. Zhang, U. Diebold, and T.E. Madey, Surf. Sci. **322**, 221 (1995).

[28] R.A. Campbell, J.A. Rodriguez, and D.W. Goodman, Surf. Sci. **240**, 71 (1990).

[29] F.A. Shunk and M. Hansen, *Constitution of Binary Alloys, 2nd Supplement* (McGraw-Hill, New York, 1969).

[30] R.P. Elliot and M. Hansen, *Constitution of Binary Alloys, 1st Supplement* (McGraw-Hill, New York, 1965).

[31] R.E. Watson and L.H. Bennett, Phys. Rev. Lett. **143**, 1130 (1979).

[32] R.E. Watson, L.J. Swartzendruber, and L.H. Bennett, Phys. Rev. B **24**, 6211 (1981).

[33] C. Froese-Fischer, *The Hartree-Fock Method for Atoms: a Numerical Approach* (Wiley, New York, 1977).

[34] M. Weinert, J.W. Davenport, and R.E. Watson, Phys. Rev. B **34**, 2971 (1986).

[35] G.G. Kleiman and R. Landers, J. Electron Spectrosc. Relat. Phenom. **76**, 310 (1995).

[36] M. Weinert and R.E. Watson, Phys. Rev. B **51**, 17 168 (1995).

[37] R.E. Watson, J.W. Davenport, and M. Weinert, Phys. Rev. B **36**, 6396 (1987).

[38] N. Martensson, A. Stenborg, O. Bjornholm, A. Nilsson, and J.N. Andersen, Phys. Rev. Lett. **60**, 1731 (1988).

[39] A. Christensen, A.V. Ruban, P. Stoltze, K.W. Jacobsen, H.L. Skriver, and J.K. Norskov, Phys. Rev. B **56**, 5822 (1997).

[40] P. Steiner, S. Hufner, N. Martensson, and B. Johansson, Solid State Commun. **37**, 73 (1981).

[41] A.R. Miedema, Physica B & C **100B**, 1 (1980).

[42] O.K. Andersen, Phys. Rev. B **2**, 883 (1970).

[43] A. Bzowski and T.K. Sham, Phys. Rev. B **48**, 7836 (1993).

[44] R.E. Watson, M. Weinert, J.W. Davenport, and G.W. Fernando, Phys. Rev. B **39**, 10 761 (1989).

[45] G.W. Fernando, R.E. Watson, and M. Weinert, Phys. Rev. B **45**, 8233 (1992).

[46] X-H. Pan, M.W. Ruckman, and M. Strongin, Phys. Rev. B **35**, 3734 (1987).

[47] M.W. Ruckman, V. Murgai, and M. Strongin, Phys. Rev. B **34**, 6759 (1986).

[48] R.E. Watson, J.W. Davenport, and M. Weinert, Phys. Rev. B **34**, 8421 (1986).

[49] M. Strongin, M.W. Ruckman, M. Weinert, R.E. Watson, and J.W Davenport, in *Metallic Alloys: Experimental and Theoretical Perspectives*, edited by J.S. Faulkner and R.G. Jordan (Kluwer, Boston, 1994), p. 37.